Ecosystems (2022) 25: 44–60
https://doi.org/10.1007/s10021-021-00639-3

Warming Stimulates Iron-Mediated Carbon and Nutrient Cycling in Mineral-Poor Peatlands

Holly J. Curtinrich,[1] Stephen D. Sebestyen,[2] Natalie A. Griffiths,[3] and Steven J. Hall[1]*

[1]*Department of Ecology, Evolution, and Organismal Biology, Iowa State University, Ames, Iowa, USA;* [2]*Northern Research Station, USDA Forest Service, Grand Rapids, Minnesota 55744, USA;* [3]*Climate Change Science Institute and Environmental Sciences Division, Oak Ridge National Laboratory, Oak Ridge, Tennessee 37831, USA*

Abstract

Iron (Fe) plays a key role in elemental cycling at terrestrial–aquatic interfaces by stabilizing carbon (C), phosphorus (P), and nutrient cations through physicochemical associations and by potentially releasing these elements following the reduction of Fe(III) to Fe(II). However, the ecosystem-scale importance of Fe redox cycling and its responses to climate change remain unclear in precipitation-fed peatlands (bogs), C-rich wetlands with very low mineral content. We tested impacts of Fe redox cycling on C and nutrient release in two bogs in northern Minnesota and in Spruce and Peatland Responses Under Changing Environments (SPRUCE), an ecosystem-scale warming experiment. Concentrations of Fe(III) declined from the peat surface to 50 cm depth (31 to 0.5 μmol g^{-1}) and co-occurred with Fe(II) (10 to 30 μmol g^{-1}). Chemical reduction of Fe(III) released C and P from variably saturated (0–30 cm) peat (106–1006 μmol C g^{-1}; 0.6–5 μmol P g^{-1}), and Fe-bound C was similar to previous measurements from upland mineral soils. Concentrations of Fe(II) and dissolved organic carbon (DOC) were strongly (R^2 = 0.56–0.78) and positively correlated in water samples measured at SPRUCE enclosure outlets and ambient near-surface porewater. Concentrations of Fe(II) also correlated positively with P at warmer SPRUCE temperature treatments and increased with experimental warming, but stabilized at the highest temperature treatments as water depth declined. Although bogs have low total mineral content, mass balance measurements indicated that atmospheric deposition could in principle sustain significant Fe cycling and hydrologic losses in these ecosystems. Overall, Fe redox cycling significantly impacted C and nutrient dynamics in these mineral-poor bogs, contributing to strong correlations between Fe(II) and DOC in water samples. Increased Fe(III) reduction with warmer temperatures will likely promote peatland C and nutrient release, impacting ecosystem C budgets both directly and indirectly by enhancing decomposition and productivity.

Key words: Bog; DOC; Iron; Marcell Experimental Forest; Mineral-associated carbon; Phosphorus; Redox.

Received 27 October 2020; accepted 25 March 2021;
published online 4 May 2021

Supplementary Information: The online version contains supplementary material available at https://doi.org/10.1007/s10021-021-00639-3.

Author Contributions: All authors performed research; HJC and SJH conceived of the study, analyzed data, and wrote the paper with contributions from SDS and NAG.

**Corresponding author; e-mail:* stevenjh@iastate.edu

Highlights

- Iron mediates carbon and nutrient stabilization and mobilization in mineral-poor peatlands.
- Temperature and soil moisture regulate iron reduction (iron(III) to iron(II)).
- Iron(II) strongly correlates with dissolved organic carbon in bog surface water.

Introduction

Iron (Fe) interacts with carbon (C) and nutrients in soil and water via multiple functional roles (McKnight and Bencala 1990; Kleber and others 2015; Chen and others 2020). Iron-C associations that stabilize C include physical interactions, such as aggregation, and chemical bonding, such as sorption and co-precipitation (Kleber and others 2015; Wagai and Mayer 2007; Zhao and others 2016). However, changes in Fe redox state can also cause C loss. Reduction of Fe(III) to Fe(II) in anoxic environments sustains microbial respiration while also potentially releasing Fe-bound C, which may be leached or decomposed (Thompson and others 2006; Pan and others 2016; Chen and others 2020). Similarly, while Fe can sorb and limit phosphorus (P) availability, P may be released when Fe(III) is reduced (Chacon and others 2006). Cations such as calcium (Ca), potassium (K), and magnesium (Mg) may also be associated with Fe-bound organic matter and released following Fe(III) reduction (Hall and Huang 2017). However, Fe-C-nutrient interactions have been primarily studied in mineral soils, and the importance of Fe as a biogeochemical driver in mineral-poor peatlands remains unclear.

Peatland Fe concentrations may vary along a hydrologic continuum from groundwater-fed fens to precipitation-fed bogs. In fens, Fe concentrations can be high enough that Fe is an important terminal electron acceptor under anoxic conditions (Küsel and others 2008) and can protect C via co-precipitation under oxic conditions (Riedel and others 2013). In contrast, raised bogs are typically isolated from a groundwater source and have lower peat Fe than fens (Urban and others 2011; Herndon and others 2019). Iron(III) reduction was therefore thought to have a minor influence on C mineralization in bogs (Blodau and others 2002; Keller and Bridgham 2007), where solid-phase organic matter may provide a much larger microbial electron sink (Keller and Takagi 2013). Furthermore, some Fe(III) may be unavailable for microbial reduction due to complexation with soil organic matter (Senesi and others 1977). However, even small amounts of Fe might still have significant impacts on other aspects of C and nutrient cycling, such as dissolved organic carbon (DOC) or P availability. For instance, Fe can limit P availability in both bogs and fens (Herndon and others 2019), where P is often a limiting nutrient (Bridgham and others 1996; Hill and others 2014). Additionally, because DOC leaching is typically a large C flux in peatlands relative to net ecosystem exchange (Griffiths and others 2017), impacts of a small Fe pool on DOC retention in the solid phase versus release to the aqueous phase may be ecologically important.

Bogs have temporally dynamic water tables that may drive seasonal redox fluctuations that dissolve and precipitate Fe along with C and nutrients. Water levels in surface peat fluctuate on seasonal and annual scales (Sebestyen and others 2011a; Griffiths and others 2019), leading to variable oxygen (O_2) availability. Iron can coprecipitate with DOC at redox interfaces when anoxic porewater is oxidized (Riedel and others 2013). These coprecipitates may dissolve if Fe(III) is reduced when the soil becomes anoxic again (Thompson and others 2006; Pan and others 2016; Chen and others 2020). If Fe reduction and oxidation are important controls on peatland DOC release, we would expect correlations between Fe and DOC in water samples from peatland catchments. Elsewhere, positive correlations between Fe and DOC have been observed in water from streams and lakes (Neal and others 2008; Knorr 2013; Oni and others 2013; Weyhenmeyer and others 2014), and porewater from freshwater estuaries (Chin and others 1998) and fens (Knorr 2013), among other ecosystems. However, multiple mechanisms could explain these relationships, and it is possible that Fe might be a ''passenger'' as well as a driver of DOC loss. Iron(III) could be stabilized in solution by DOC through complexation (Blazevic and others 2016) or bound to C as microparticulate Fe(III) (Neal and others 2008). Iron and DOC could both be responding to another driver, such as pH change due to decreasing sulfur deposition (Neal and others 2008; Björnerås and others 2017). Finally, Fe(II) may be protected from oxidation by complexation with DOC (Theis and Singer 1974; Daugherty and others 2017) and thus co-transported with DOC. Measurements of Fe redox state in water samples could provide further mechanistic insight into relationships between Fe and DOC, or the lack thereof (for example, Ekström and others 2016).

In peatlands, it is also uncertain how changes in temperature or moisture expected under future

climates may influence coupled Fe-C-nutrient dynamics. Laboratory experiments indicate that warming increases Fe(III) reduction (Yao and Conrad 2000; Meier and others 2005; Schilling and others 2019), but we are not aware of experiments testing the temperature sensitivity of Fe(III) reduction at ecosystem scale. Temperature and water depth may interactively control Fe(III) reduction in peatlands. High water levels limit diffusion of O_2 into surface peat, but may not lead to microbial O_2 consumption and Fe(III) reduction when temperature is low. Conversely, elevated temperatures stimulate microbial activity but lead to increased evapotranspiration and lower peatland water levels (Hanson and others 2020a), potentially limiting Fe(III) reduction. The interactive effects of water level and temperature on Fe(III) reduction could impact retention or loss of C and nutrients in peatlands and other wetland ecosystems.

Here, we asked whether Fe influences C and nutrient cycling, and how temperature and moisture affect these processes, using measurements from two bogs in the Marcell Experimental Forest, MN (Kolka and others 2011) and the SPRUCE ecosystem warming and CO_2-enrichment experiment (Hanson and others 2017). We hypothesized that Fe(III) reduction leads to release of DOC and soluble P in peat and catchment outflow. To test this, we quantified Fe, Fe-bound C, and other ions released by Fe(III) reduction in peat core extractions, and measured Fe(II), Fe(III), total organic carbon (TOC), and major ions in surface water and near-surface porewater samples. To parse out multiple potential mechanisms contributing to Fe–DOC relationships in catchment water samples, we compared the correlation between DOC and Fe to the correlation between DOC and other ions. If Fe is primarily a passenger of DOC export due to evaporative concentration or electrostatic interactions, we expected that correlations between Fe and DOC would be similar to those observed for other cations and DOC in bulk water samples, and that Fe(III) would be dominantly correlated with DOC. However, if Fe is both a driver and a passenger of DOC export, we expected that the relationship between Fe and DOC would differ from other cations, and that Fe(II) would have a stronger relationship with DOC than Fe(III). We also hypothesized that Fe(II) concentrations in water measured at the outlets of SPRUCE treatment enclosures would increase with temperature, contingent on saturated conditions.

Methods

Site Description

Samples were collected from two boreal peat bogs, denoted S1 and S2, that are about 1.5 km apart in the Marcell Experimental Forest (near Grand Rapids, MN, USA; 93.472° W, 47.504° N and 93.473° W, 47.514° N, respectively) (Sebestyen and others 2021b). From 1961 to 2019, mean annual precipitation was 78.7 cm and mean annual temperature was 3.6 °C (Sebestyen and others 2021b). The S1 bog has an area of 8.1 ha, a maximum elevation of 430 m, and an outlet elevation of 412 m. The S2 bog has an area of 3.2 ha, a maximum elevation of 430 m, and an outlet elevation of 420 m (Sebestyen and others 2011a). Both bogs are acidic, with pH values near 4 (Griffiths and Sebestyen 2016; Sebestyen and others 2021a), and ombrotrophic, with precipitation as the dominant water source (Verry 1975). Each bog is drained by an intermittent stream (Sebestyen and others 2011a; Verry and others 2011). Vegetation consists mostly of black spruce (*Picea mariana*), *Sphagnum* moss, and ericaceous shrubs (Sebestyen and others 2011a). Trees in the S1 bog were experimentally felled in 1969 and 1974 with no effect on bog water table or stream water yield (Sebestyen and others 2011b). The S2 bog has been used as a reference peatland for experiments at surrounding sites (Sebestyen and others 2011a).

The S1 bog is the location of the SPRUCE experiment, where above- and below-ground warming and elevated CO_2 treatments are applied in a regression design to 12.8-m diameter open-top enclosures (Hanson and others 2017). Five temperature treatments, + 0 °C, + 2.25 °C, + 4.5 °C, + 6.75 °C, and + 9 °C above ambient, were each applied to two enclosures, and one of each temperature level received elevated CO_2 at + 500 ppm above ambient (Hanson and others 2017). Peat temperature profiles were measured at three zones within each enclosure (Hanson and others 2016, 2017). Warming treatments achieved air and deep peat temperature values very close to the targets (Hanson and others 2017), so we used nominal temperature values as predictors in statistical analyses. We favored nominal temperatures due to heterogeneity of measured soil moisture and temperature and uncertainty about depths where Fe(III) reduction occurred. However, we also report mean 5 cm peat temperature measured in each enclosure during the period of water sample collection. The enclosures are hydrologically separated by a below-ground wall (''corral'') to prevent water

inflow from the surrounding peatland. Natural, passive drainage of the enclosed space occurs via two shallow lateral pipes, with drainage to a reservoir where water is autosampled and volumetric water measurements are made (Sebestyen and Griffiths 2016). Each enclosure and outflow is conceptually analogous to a zero-order stream that drains from an entire peatland (Sebestyen and Griffiths 2016). Flow is intermittent, and largest flows typically occur during spring snowmelt.

Peat Sampling and Analyses

We sampled two peat cores from each bog in September 2017 with a stainless-steel Russian corer (5 cm diameter; Eijelkamp Agrisearch Eqiupment, Giesbeek, The Netherlands). Cores from the S1 bog were sampled outside of SPRUCE enclosures. Cores were taken from the hollow surface to 2 m depth and divided in increments of 10 cm for the first 50 cm and 25 cm thereafter. Samples were sealed in polyethylene bags, kept on ice until arrival at the field laboratory, and maintained at − 20 °C until analysis. Thawed samples were homogenized inside the bags, and subsamples (still at field moisture content) were immediately subjected to several chemical extractions and moisture and pH measurements. Gravimetric moisture content was determined by drying about 10 g at 100 °C for more than 48 h, and pH was measured by placing an electrode into an approximately 5 g aliquot of each field-moist sample (Table S2).

Concentrations of Fe(II) and Fe(III) were quantified in 0.5 M hydrochloric acid (HCl) extractions with an approximate ratio of 1:30 dry mass equivalent to solution, hereafter defined as $Fe(II)_{HCl}$ and $Fe(III)_{HCl}$, respectively. Samples were vortexed for 1 min, shaken at 120 rpm for one h on a rotary shaker, and centrifuged at 10,000 g for 10 min. The supernatant was removed by pipette and stored in the dark at 4 °C. The $Fe(II)_{HCl}$ and $Fe(III)_{HCl}$ were colorimetrically measured using a ferrozine method which is robust to high concentrations of co-occurring DOC (Huang and Hall 2017b). This method has long been used to measure redox-sensitive Fe pools in sediment and soil: the low pH of 0.5 M HCl inhibits Fe(II) oxidation and extracts dissolved and sorbed Fe(II) and Fe(III), along with a highly reactive fraction of Fe(III) solid phases (Lovley and Phillips 1987). The 0.5 M HCl extraction also may release Fe(II)-bearing phases such as siderite and magnetite (Chen and others 2018), but these were not likely present (Herndon and others 2019). Peat often contains reduced organic moieties (''humics'') that can transfer electrons to Fe(III) (Keller and Takagi 2013). This process is favored as pH decreases, likely due to increased Fe(III) solubility or shifts in the potentials of the humic and Fe redox couples (Chen and others 2003). Therefore, the low pH of the 0.5 M HCl extraction might cause additional chemical Fe(III) reduction coupled to humic oxidation. However, 0.5 M HCl-extractable Fe(III) persists even in anoxic soils rich in soluble polyphenolics (Hall and others 2014; Chen and others 2020), indicating that the extraction per se does not necessarily reduce Fe(III) to Fe(II). In any case, the 0.5 M HCl extraction represents a conservative metric of Fe(III) that is vulnerable to dissimilatory reduction (Lovley and Phillips 1987).

Additional field-moist peat subsamples were extracted with 0.05 M sodium dithionite in a ratio of 1:180 dry mass equivalent to solution. This extraction reduces Fe(III) to Fe(II), releasing C that was directly or indirectly associated with Fe(III). In principle, dithionite solubilizes the entire Fe(III) pool, unless it is shielded from reductive dissolution by other minerals or organics (Senesi and others 1977). Samples were vortexed for 1 min, shaken for 16 h, and centrifuged for 10 min at 20,000 g. The supernatant was removed and residues were further extracted with 0.05 M HCl to dissolve any Fe that may have precipitated with sulfides (Wagai and Mayer 2007). Separate subsamples were extracted with 0.05 M sodium sulfate to account for any organic C released following ion exchange with sulfate, the oxidation product of dithionite (Wagai and Mayer 2007). We also measured Fe in the sulfate extractions, interpreted as the soluble or weakly exchangeable Fe pool. The dithionite and sodium sulfate extractions were conducted in parallel on replicate subsamples, not sequentially, due to the difficulty of completely removing the solution without removing the peat. The dithionite and sulfate extractions were acidified to approximately pH 2 with HCl to inhibit microbial activity before storage at 4 °C. The Fe in these extractions was measured with ferrozine as described above, denoted as Fe_{d+HCl} and Fe_s, respectively. We calculated Fe_{d+HCl} as the sum of Fe in the dithionite and the subsequent HCl extraction after accounting for Fe remaining in the residual supernatant.

The DOC in the dithionite and sulfate extractions was determined by wet oxidation following Huang and Hall (2017a). Solutions were combined with powdered potassium persulfate as an oxidant, acidified with phosphoric acid, and sealed in gastight vials. Samples were bubbled with CO_2-free air to remove dissolved inorganic carbon and head-

space CO_2 and heated to 102 °C on a block heater to oxidize DOC to CO_2, which was measured by injection into a tunable diode laser (Campbell Scientific TGA200A, Logan UT). We refer to DOC measured in the dithionite and sulfate reactions as DOC_d and DOC_s, respectively, and Fe-associated C is calculated as their difference (Wagai and Mayer 2007). We expressed Fe and DOC on a volume basis using bulk density data from cores sampled previously in the S1 bog (Iversen and others 2014). We measured Ca, Mg, Fe, K, P, and aluminum (Al) in the dithionite + HCl, dithionite, and sulfate extractions with inductively coupled plasma optical emission spectrometry (ICP-OES; PerkinElmer Optima 5300 DV, Waltham, MA). Iron was measured by ICP-OES to further validate the colorimetric method used in the other analyses.

Water Sample Collection/Analysis

Water samples were collected periodically from October 2016 to November 2018 at the outflows of the SPRUCE enclosures (n = 55–70 per enclosure) and from September 2016 to October 2018 in near-surface porewater (0–10 cm) of the S2 bog at three different sampling sites, KF45, KF45A, and KF5A (n = 31–69 per site). The KF45 and KF45A sites were located near the bog center and KF5A was at the southern boundary. The Fe(II) and total Fe in these samples were measured with ferrozine as described above. We calculated Fe(III) as the difference between total Fe and Fe(II), which gave small negative values for several samples with extremely low Fe(III). We defined the absolute value of these negative numbers as a conservative detection limit for Fe(III) (1.2 μM) and set positive Fe(III) values within this range to zero. Total organic C (TOC) was analyzed by wet combustion to CO_2 (Shimadzu VCP, Columbia, MD); TOC is equivalent to DOC in this ecosystem (Sebestyen and others 2020a) and will hereafter be referred to as DOC. Soluble reactive phosphorus (SRP) was measured using the antimony-molybdate method on a Lachat QuickChem 8000, sulfate and chloride were measured using ion chromatography (with suppressed conductivity detection) on a Thermo Scientific Dionex ICS-2100, and Ca and Na were measured using inductively coupled plasma optical emission spectrometry (ICP-OES) on a Thermo Elemental ICP-OES Icap 7600 Duo. The water sample data for the S2 bog, the SPRUCE outflows, and the peat data used in this paper have been published separately (Sebestyen and others 2021b, 2021c, Curtinrich and others 2021).

Mass Balance of Fe

The average outflow of Fe (yield, g m^{-2} y^{-1}) over 2017 and 2018 from the SPRUCE enclosures was estimated based on total Fe concentrations (Fe(II) + Fe(III)) and water discharge data (Table S1). Iron concentrations were linearly interpolated between measurement dates. Peat Fe stocks were calculated from mean Fe_{d+HCl} mass concentrations and S1 bulk density values (Iversen and others 2014). Iron residence time was calculated as Fe stock divided by Fe yield from each enclosure.

Data Analysis

We assessed pairwise relationships between DOC and ions using linear regression with interaction terms to test for differences among SPRUCE nominal temperature treatments and S2 sampling locations. We used SPRUCE enclosure as a random effect to account for autocorrelations among measurements from a given enclosure. To account for nonlinear trends in response variables, we fit generalized additive mixed models (GAMMs) using the gamm function in the mgcv package in R (Wood 2006), with enclosure as a random effect. As GAMM predictors, we separately used nominal temperature treatments and the empirically measured mean 5 cm peat temperature for each enclosure (Hanson and others 2016). We also tested the significance of CO_2 treatment as a categorical predictor. Additionally, we applied GAMMs to assess temporal trends in SPRUCE Fe(II) with 5 cm peat temperature (Hanson and others 2016) and water table elevation (Hanson and others 2020b) with and without interaction; optimum models were selected by comparing Akaike's Information Criterion (AIC) values. Water depth was normalized to mean hollow elevation (Hanson and others 2020b). To test for presence of significant Fe-associated C or differences between pools, we used paired t tests at each depth. Each individual core was used as replicate as cores showed similar trends. All analyses were done using R version 3.5.3 and $\alpha = 0.05$.

Results

Peat Profile Chemical Composition

Extractable Fe showed relatively consistent trends with depth among the four peat cores from the two bogs. Mass concentrations of Fe_{d+HCl} and Fe_{HCl} tended to be greatest at the surface and declined with depth but exhibited a secondary maximum at

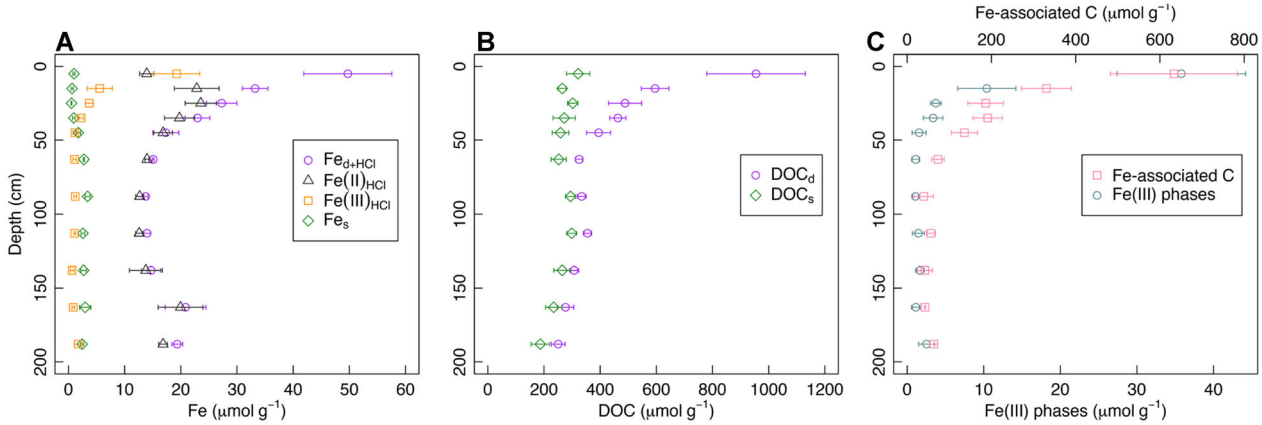

Figure 1. Depth profiles of mean Fe_{d+HCl}, Fe_s, $Fe(II)_{HCl}$, and $Fe(III)_{HCl}$ concentrations (**A**), mean DOC_d and DOC_s concentrations (**B**), and mean Fe-associated C and Fe(III) phases (**C**) in peat collected from two bogs. We calculated Fe-associated C as DOC_d–DOC_s and Fe(III) phases as Fe_{d+HCl}–$Fe(II)_{HCl}$. Error bars show the standard error of the mean (n = 4).

150–175 cm (Figure 1A; Table S2). The concentration of $Fe(II)_{HCl}$ was significantly greater than $Fe(III)_{HCl}$ for most depths ($P < 0.05$), except 0–20 cm, where they were equivalent. The concentration of $Fe(III)_{HCl}$ was greatest at 0–10 cm (19.3 ± 4.1 μmol g^{-1}, mean ± SE), below which $Fe(III)_{HCl}$ concentrations decreased (0–12.1 μmol g^{-1}) but were still significantly greater than zero for depths 20–125 cm and 150–175 cm ($P < 0.05$; Figure 1A). In contrast, $Fe(II)_{HCl}$ tended to be highest at 20–30 cm, as well as deeper in the profile (150–175 cm). Concentrations of Fe_{d+HCl} were significantly greater than Fe_{HCl} at the surface (0–10 cm; $P < 0.05$) but were similar throughout the rest of the profile (Table S2). Concentrations of Fe_s were significantly smaller than Fe_{d+HCl} ($P < 0.01$) and Fe_{HCl} ($P < 0.05$) but were still significantly greater than zero at all depths except for 150–175 cm ($P < 0.05$). Trends of Fe with depth were slightly different when calculated on a volume vs. mass basis (Figures 1A, S1a). On a volume basis, Fe_{d+HCl} was lower at the surface and peaked at 30–40 cm and 175–200 cm (Figure S1a). Mean volumetric $Fe(II)_{HCl}$ peaked at 30–40 cm and 150–175 cm, compared to 20–30 cm when measured on a mass basis. The volumetric trends of $Fe(III)_{HCl}$ and Fe_s were similar to those on a mass basis, except the peak of $Fe(III)_{HCl}$ at the surface was less pronounced.

The difference in DOC concentrations between the dithionite (DOC_d) and sulfate extractions (DOC_s) reflects Fe-associated C released to solution following reductive dissolution of any Fe(III). The mean Fe-associated C concentration was greatest at 0–10 cm (633 ± 151 μmol g^{-1}) and declined with depth to 73 ± 15 μmol g^{-1} at 50–75 cm and 64 ± 9.2 μmol g^{-1} at 175–200 cm (Figure 1C). Although Fe-associated C was lower at depth, DOC_d was significantly greater than DOC_s at all depths ($P < 0.05$) except for 75–100 cm and 125–150 cm, where they were equivalent (Figure 1B). On a volume basis, mean DOC_d was greatest near 30–40 cm (Figure S1b). Mean Fe-associated C was 29.6 ± 7.1 μmol cm^{-3} at the surface but increased slightly to 32.2 ± 5.8 μmol cm^{-3} at 30–40 cm before decreasing with depth (Figure S1c).

Concentrations of P, Mg, K, Fe, Ca, and Al in dithionite + HCl, dithionite, and sulfate extractions showed different trends with depth (Figure 2). Concentrations of P_{d+HCl} and P_d were significantly greater than P_s at 0–30 cm ($P < 0.05$; Figures 2E, S2c) and were similar below 30 cm. Overall, all three extractions of P, Mg, and K were higher at the surface and decreased to about 50 cm, below which they remained consistent with depth (Figure 2). Concentrations of Mg_{d+HCl} were significantly higher than Mg_s for all depths except 100–125 cm ($P < 0.05$; Figures 2B, S2b) and Mg_d was significantly higher than Mg_s for all depths except 50–75 cm and 100–125 cm ($P < 0.05$). Iron (Fe_{d+HCl} and Fe_s) showed the same trends when measured on the ICP (Figure 2B) as when measured colorimetrically (Figure 1A). In contrast to the other elements, Ca did not show a trend with depth for any extraction. Concentrations of Ca_{d+HCl} were significantly greater than Ca_s at 20–50 cm, 75–100 cm, and 125–200 cm ($P < 0.05$; Figures 2A, S2a). Also, in contrast to the other elements, Al_{d+HCl} and Al_d concentrations steadily increased with depth while Al_s remained consistently low.

Relationships Between Ions and DOC in Water Samples

Water samples from the SPRUCE enclosures and the S2 bog showed strong linear correlations between Fe(II) and DOC (Figure 3A, C; regression details are provided in Table 1 and are provided in the figure captions for subsequent regressions). The slope of the relationship between Fe(II) and DOC did not vary among SPRUCE temperature treatments (i.e., there was no significant slope x temperature interaction; Figure 3A, Table 1). Similarly, the slope of the relationship between Fe(II) and DOC did not significantly differ among S2 bog sampling sites (Figure 3C, Table 1). In contrast, Fe(III) did not correlate with DOC in the SPRUCE water samples (Figure S3a). Furthermore, there was a negative relationship between Fe(III) and DOC for two of the S2 sites ($P < 0.05$ and $P < 0.001$) and an insignificant relationship for the third site (Figure S3b).

Calcium also showed a positive linear relationship with DOC in the SPRUCE enclosure outflow samples and in the S2 bog porewater. In contrast to Fe(II), however, the slope of the relationship between Ca and DOC strongly varied among SPRUCE temperature treatments ($P < 0.0001$; Figure 3B, Table 1) and between S2 sampling sites ($P < 0.0001$; Figure 3D, Table 1). The slope of the regression line between Ca (predictor variable) and DOC (response variable) became steeper with temperature until + 4.5 °C and then became shallower at the higher temperature treatments (Figure 3B, Table 1). Similar to Ca, the slope of the relationship between Na and DOC also changed among temperature treatments ($P < 0.0001$; Figure S4a). Most of the temperature treatments showed a significant linear correlation between Na and DOC, and the slope of the regression lines became progressively steeper with higher temperature (Figure S4a). There was also a significant linear correlation between Na and DOC in the S2 bog which did not change between sampling sites (Figure S4b). Chloride also showed a weak ($R^2 = 0.09$) but significant ($P < 0.0001$) positive linear relationship with DOC in the SPRUCE

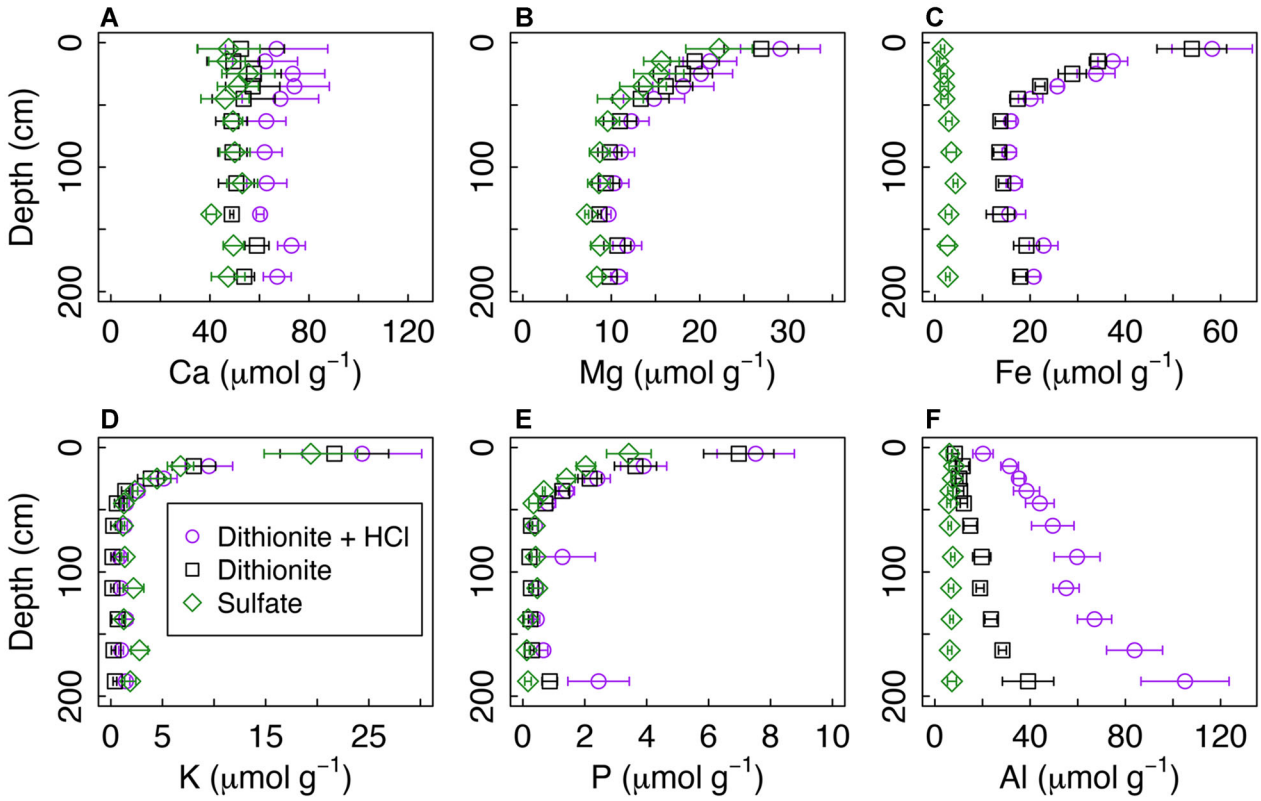

Figure 2. Depth profiles of mean Ca (**A**), Mg (**B**), Fe (**C**), K (**D**), P (**E**), and Al (**F**) concentrations in the dithionite + HCl, dithionite, and sulfate extractions in peat collected from two bogs. The error bars show standard error of the mean ($n = 4$, except K_{d+HCl} depths 88, 113, and 163 cm where $n = 3$). The Fe (**B**) shown here was measured on the ICP and used to verify the colorimetric method (Figure 1).

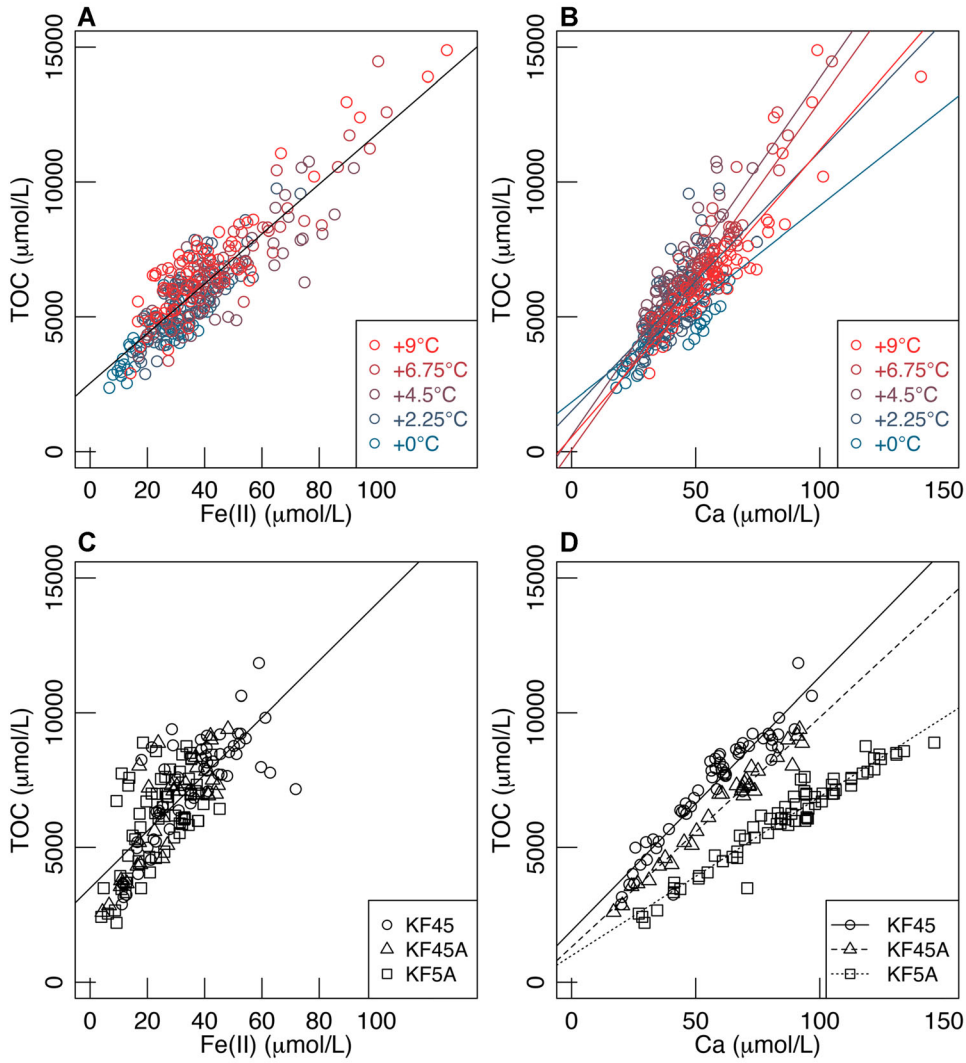

Figure 3. Pairwise relationships between TOC and Fe(II) in the water samples from the SPRUCE enclosure outflows (**A**) and the S2 bog (**C**) and pairwise relationships between TOC and Ca in the water samples from the SPRUCE enclosure outflows (**B**) and the S2 bog (**D**). Colors represent SPRUCE temperature treatments + 0 °C, + 2.25 °C, + 4.5 °C, + 6.75 °C, + 9 °C (**A**, **B**), and the black circles, diamonds, and squares represent the S2 sites KF45, KF45A, and KF5A, respectively (**C**, **D**). The regression details for Figure 3 can be found in Table 1.

enclosure outflow samples which did not vary significantly among SPRUCE temperature treatments (Figure S5a). Chloride did not show a significant correlation with DOC in the S2 bog samples (Figure S5b). Concentrations of sulfate in the SPRUCE (2.3 ± 0.1 µmol L^{-1}) and S2 (2.1 ± 0.1 µmol L^{-1}) samples were low compared to Fe and did not correlate significantly with DOC (Figure S6a, b).

Relationships Between Fe and SRP in Water Samples

Concentrations of SRP measured 3.5 ± 0.3 µmol L^{-1} (mean ± SE) in the SPRUCE samples and 0.9 ± 0.1 µmol L^{-1} in the S2 samples. The relationship between SRP and Fe(II) shifted from a negative correlation at ambient temperatures in S2 and an insignificant relationship at low SPRUCE temperature treatments to a positive correlation at higher SPRUCE temperatures (significant slope x temperature interaction, $P < 0.0001$; Figure S7a, b). The strongest relationship between Fe(II) and SRP in the SPRUCE samples occurred in the + 6.75 °C treatment ($R^2 = 0.32$, $P < 0.0001$). We found a weakly significant negative linear correlation between Fe(II) and SRP in the S2 bog ($R^2 = 0.07$, $P < 0.01$; Figure S7b).

Table 1. Summary Statistics for Figure 3 Regressions.

Site/treatment	Equation[a]	R^2	*P* value	*F* statistic	Model Df	Error Df
SPRUCE	TOC = 92.3 (± 2.7) Fe(II) + 2534.1 (± 115.6)	0.78	< 0.0001	1157	1	324
SPRUCE + 0	TOC = 72.8 (± 6.7) Ca + 1840.9 (± 272.2)	0.63	< 0.0001	117	1	68
SPRUCE + 2.25	TOC = 96.3 (± 14.1) Ca + 1512.2 (± 632.5)	0.42	< 0.0001	47	1	65
SPRUCE + 4.5	TOC = 132.6 (± 9.2) Ca + 597.8 (± 405.3)	0.76	< 0.0001	209	1	65
SPRUCE + 6.75	TOC = 129.2 (± 6.3) Ca + 70.0 (± 345.4)	0.87	< 0.0001	425	1	65
SPRUCE + 9	TOC = 106.4 (± 7.1) Ca + 544.2 (± 451.0)	0.81	< 0.0001	227	1	53
S2	TOC = 105.4 (± 7.6) Fe(II) + 3497.9 (± 244.4)	0.56	< 0.0001	194	1	155
S2 KF45	TOC = 94.1 (± 4.4) Ca + 1916.0 (± 264.5)	0.89	< 0.0001	458	1	55
S2 KF45A	TOC = 85.2 (± 2.5) Ca + 1312.0 (± 162.9)	0.97	< 0.0001	1122	1	29
S2 KF5A	TOC = 58.9 (± 1.8) Ca + 988.2 (± 167.4)	0.94	< 0.0001	1031	1	66

[a]*Units for regression equations are all reported in μmol* L^{-1}.

Influence of Temperature Treatments on SPRUCE Outflow Metal and DOC Concentrations

Iron(II) concentrations in the SPRUCE outflow water samples increased at higher temperature treatments but started to plateau at + 6.75 °C (Figure 4A). This nonlinear trend approximated a smooth function with 1.9 estimated degrees of freedom (edf) in the GAMM ($P < 0.0001$). The mean Fe(II) concentration at + 6.75 °C (46.0 ± 2.4 μmol L^{-1}) was 67% higher than at + 0 °C (27.5 ± 1.3 μmol L^{-1}; Table S3). A similar result was obtained when measured mean 5 cm peat temperature values were used instead of the nominal temperature treatments ($P < 0.001$; Figure S8). Conversely, temperature treatments did not significantly affect outflow Fe(III) when assessed by either metric (nominal temperature treatment or measured peat temperature). Elevated CO_2 had an insignificant effect on Fe(II) in the GAMM with nominal temperature treatments and a small but significant negative effect of

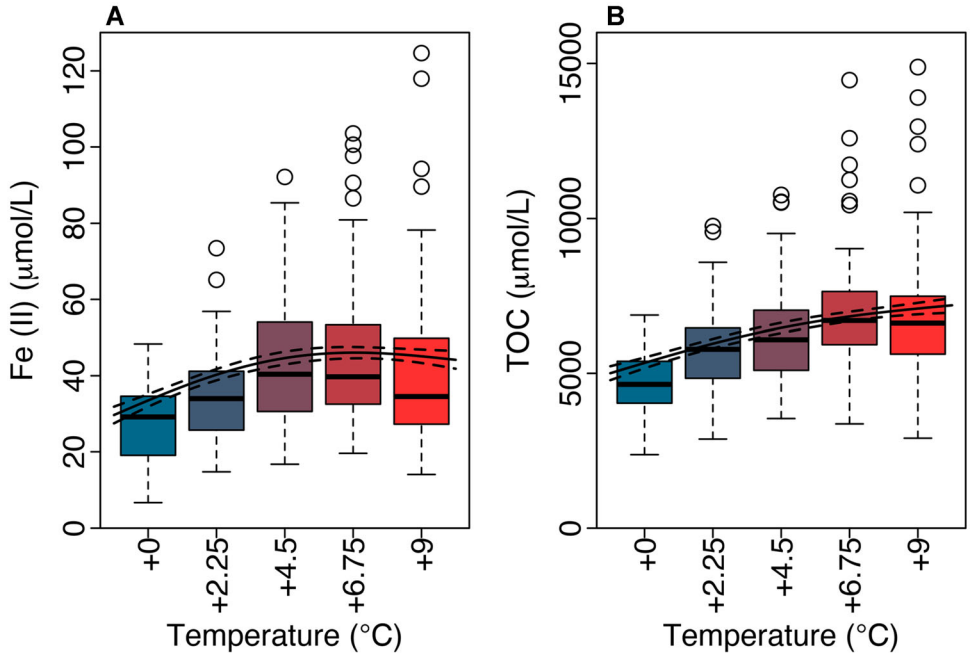

Figure 4. Fe(II) (**A**) and TOC (**B**) concentrations in water samples from the SPRUCE enclosure outflows. The solid lines represent the GAMMs with nominal temperature as the smoothing variable, and the dotted lines represent the standard error of the smooth function. GAMM for Fe(II): R^2 (adj) = 0.14, $P < 0.0001$, F = 19. 95, edf = 1.9, Ref df = 1.9 (**A**). GAMM for TOC: R^2 (adj) = 0.20, $P < 0.0001$, F = 31.5, edf = 1.7, Ref df = 1.7 (**B**).

-6.1 ± 2.4 μmol L^{-1} ($P < 0.05$) on Fe(II) when assessed using measured 5 cm peat temperature. Outflow concentrations of DOC showed a similar response to temperature treatment as Fe(II) except they did not plateau as much at the highest temperature treatment (Figure 4B). This nonlinear trend of DOC was shown as a smooth function with 1.7 edf in the GAMM ($P < 0.0001$). The response of outflow Ca concentrations to temperature treatments differed from Fe(II); Ca remained similar among the + 0 °C, + 2.25 °C and + 4.5 °C treatments but increased at + 6.75 °C and + 9 °C instead of plateauing. As with Fe(II), temperature also had a significant nonlinear effect on the Fe(II)/Ca molar ratio, estimated by a smooth function with 1.9 edf ($P < 0.01$; Figure S9). The Fe(II)/Ca molar ratio was greatest in the + 4.5 °C treatment and decreased at higher temperatures.

Temporal Trends and Drivers of Fe in SPRUCE and S2

When plotted over time, Fe(II) in both the SPRUCE samples and ambient S2 bog samples showed a similar pattern of increasing concentrations in spring and summer and decreasing concentrations in fall (Figure 5A, B). The optimum GAMM for temporal variation in SPRUCE Fe(II) included measured 5 cm peat temperature, water table elevation, and their interaction. Peat temperature and water table elevation had significant nonlinear effects on SPRUCE Fe(II) which were represented as smooth functions with an interaction (edf = 6.5, $P < 0.0001$, $R^2 = 0.4$). SPRUCE Fe(II) concentrations were greatest when peat temperature and water table elevation were both high (Figure 6).

The Fe yield from each of the SPRUCE enclosures over 2017 and 2018 measured 0.5–1 g m^{-2} y^{-1} (Table S4). Total reactive Fe in the enclosures measured 38 g m^{-2} from 0 to 30 cm (the acrotelm) and 269 g m^{-2} from 30 to 200 cm (the catotelm). If all Fe in the SPRUCE enclosure outflows came from the top 30 cm of peat, the steady-state residence time of Fe would be 39–82 y. If Fe in the SPRUCE outflows came equally from 0 to 200 cm, the residence time of Fe in profile would be 318–661 y.

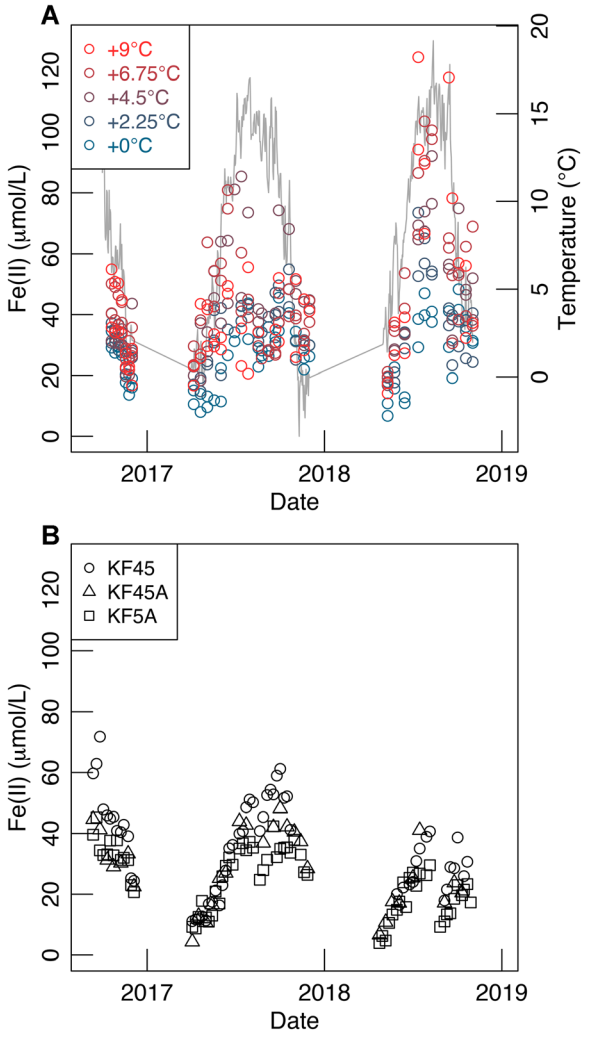

Figure 5. Fe(II) concentrations over time in the SPRUCE enclosure outflows (**A**) and the S2 bog (**B**). The different colored circles represent the SPRUCE temperature treatments (**A**) and the black circles, diamonds, and squares represent the S2 sites KF45, KF45A, and KF5A, respectively (**B**). The gray line shows peat temperature at 5 cm depth in the + 0 °C ambient CO_2 SPRUCE enclosure (**A**).

Discussion

Our results show the biogeochemical importance of Fe redox cycling in two predominantly precipitation-fed bogs, ecosystems with low total mineral content where redox-active metals have received little attention (Herndon and others 2019). Peat extractions showed the presence of substantial Fe-associated C and nutrients, particularly in the top 50 cm, that were released to solution when Fe(III) was reduced (Figure 1C). This release of C indicates that Fe could be both protecting and/or regulating the availability and losses of C and nutrients through redox cycling. A tight coupling between Fe and C was observed in water samples from the SPRUCE enclosure outflows as well as in ambient water samples from the nearby S2 bog (Figure 3A, C, Table 1). Warming has long been thought to increase peatland DOC loss by stimulating enzymatic depolymerization of organic matter (Freeman and others 2001). Below, we present several

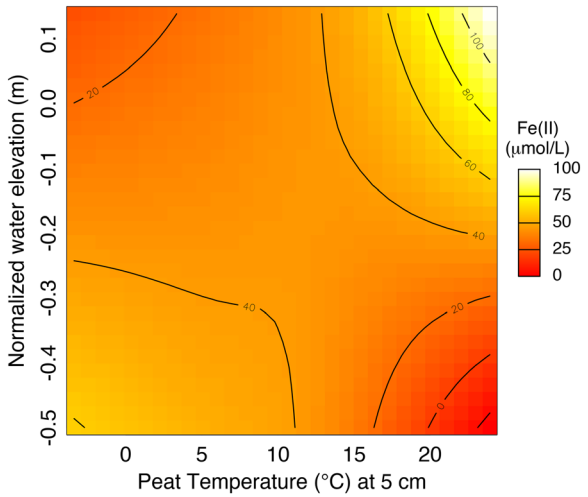

Figure 6. SPRUCE outflow water Fe(II) concentrations predicted by a GAMM with normalized water elevation and peat temperature at 5 cm below the surface, plus their interaction, as smoothing functions (R^2 = 0.4, $P < 0.0001$, F = 29.8, edf = 6.5, Ref df = 6.5). The black contour lines and color gradient show Fe(II) concentrations. Low concentrations of Fe(II) are shown in dark red, and high concentrations of Fe(II) are shown in light yellow.

lines of evidence indicating that the observed Fe(II)/DOC correlations in these water samples also partially reflect release of solid-phase C following reductive dissolution of Fe(III). However, the Fe(II)/DOC correlations also may imply that Fe was a passenger of DOC efflux due to complexation of Fe(II) by DOC. The strong response of Fe(II) to temperature and water levels in the SPRUCE treatments indicates the key role of these environmental factors in controlling Fe-mediated C cycling at the ecosystem scale (Figures 4A, 5, 6, and S8). In addition to the strong relationships between Fe and C, peat extractions and water samples pointed to the importance of Fe redox cycling in affecting P, Ca, and Mg availability.

Significant Fe and Fe-Associated C in Precipitation-Fed Ecosystems

Iron-mediated C protection is important in many mineral soils (Wagai and Mayer 2007; Kleber and others 2015; Zhao and others 2016), but its importance in mineral-poor peatlands remains unclear. Previous studies suggested that Fe was not a quantitatively important electron acceptor in other precipitation-fed peatlands (Blodau and others 2002; Keller and Bridgham 2007). At Marcell, however, we found Fe and Fe(III)-bound C concentrations similar to many upland mineral soils. The C that was chemically released from Fe(III) (that is, DOC_d—DOC_s) in the top 20 cm of Marcell peat (230–1006 μmol C g^{-1}, mean = 482 μmol C g^{-1}) was similar to measurements at the same depth from 14 disparate upland mineral forest soils (0–1607 μmol C g^{-1}, mean = 419 μmol C g^{-1}; calculated from the supplemental data of Zhao and others 2016). This similarity in Fe(III)-bound C occurred despite lower Fe_{d+HCl} in our samples (29.9–73.0 μmol Fe g^{-1}, mean = 42 μmol Fe g^{-1}) than in those forest soils (1.4–346 μmol Fe g^{-1}, mean = 76 μmol Fe g^{-1}; Zhao and others 2016). The mean Fe(III)-bound C in our samples (0–20 cm) was also similar to 30 surface soil samples from eight different soil orders measured in a separate study (0–1833 μmol g^{-1}, mean = 509 μmol g^{-1}; calculated from the supplemental material of Wagai and Mayer 2007). Those 30 soil samples also had much greater Fe_{d+HCl} than our bog samples (21–3491 μmol Fe g^{-1}, mean = 723 μmol Fe g^{-1}; Wagai and Mayer 2007). This similarity in Fe-associated C but lower Fe concentration indicates a much greater molar C/Fe ratio of Fe-associated C in our bog samples than in the soils of Zhao and others (2016) and Wagai and Mayer (2007). The higher Fe-associated C/Fe ratio in our bog samples suggests co-precipitation of Fe–C complexes, which can stabilize more C per mole Fe than sorption on Fe(III) minerals (Kleber and others 2015). Our Fe data build on findings by Herndon and others (2019), who analyzed Fe in 0–20 cm peat from hollows in the same bogs that we studied. Mössbauer spectroscopy showed that most Fe was complexed with organic matter as Fe(II) or Fe(III), and that a small pool of Fe-oxyhydroxides was present (Herndon and others 2019). Given the presence of biogeochemically relevant Fe concentrations in these organic soils, we considered what Fe sources might sustain substantial rates of Fe cycling and hydrologic losses.

The most plausible source of Fe to the bogs is dry atmospheric deposition, whereas contributions from groundwater and surface runoff are unlikely. The S1 and S2 bogs receive water from precipitation (Verry 1975), but dry deposition is a more likely Fe source (Urban and others 1987). Eisenreich and others (1978) estimated average dry Fe deposition of 0.49 g m^{-2} y^{-1} in northeast Minnesota. This is close to the average hydrologic Fe loss from the S2 bog (mean = 0.2 g m^{-2} y^{-1} over 2008–2016; Sebestyen and others, unpublished data) and from the SPRUCE enclosures (~ 0.5 to 1 g m^{-2} y^{-1}; Table S4). Bulk deposition of soluble Fe was always below the detection limit of 0.05 mg Fe L^{-1} (Sebestyen and others 2020b) such that Fe

wet deposition was at most 0.04 g m^{-2} yr^{-1} from 2010 to 2019 (the product of 0.05 mg Fe L^{-1} and annual precipitation; Sebestyen and others 2020c). Uplands contribute little if any Fe to the bogs because under saturated conditions, subsurface water from the uplands flows into a lagg (the interface between the bog and upland mineral soils) and then into the headwater stream, bypassing the bog (Verry and others 2011). Groundwater exchange is an unlikely source of Fe to the bogs because the S1 and S2 water levels are above regional groundwater by 1 and 7 m, respectively (Verry and Janssens 2011; Griffiths and Sebestyen 2016). This disparity creates a hydraulic gradient that sustains slow, deep seepage through the bottom of the bogs and laggs (Verry and others 2011). Additionally, the hydraulic conductivity of deep peat and silty clay beneath the bog is low (Verry and others 2011). Groundwater exchange might be possible over long timescales as evidenced by higher pH and Ca concentrations in deep porewater of S1 bog peat, but these differences could also represent a prior phase of peat development (Griffiths and Sebestyen 2016; Griffiths and others 2019).

Fe(III) Reduction as a Driver of the Fe–DOC Relationship

Correlations between Fe and DOC have been observed in many freshwaters (Chin and others 1998; Neal and others 2008; Knorr 2013; Weyhenmeyer and others 2014). However, such correlations have not always been observed (Ekström and others 2016; Björneråas and others 2017) and multiple possible mechanisms could contribute to Fe–C relationships in water samples. We show via multiple lines of evidence that reduction of Fe(III) in peat likely contributed to the strong observed correlation (Figure 3A, C, Table 1) between Fe(II) and DOC in the water samples from the SPRUCE enclosure outlets and in the S2 near-surface porewater. We found a release of C as DOC when Fe(III) was chemically reduced in our peat extractions (Figure 1B, C). This was consistent with observations of increased DOC following Fe(III) reduction in organic-rich mineral soils (Hagedorn and others 2000), and with incubation studies that found Fe(III) reduction led directly or indirectly to DOC release (Thompson and others 2006; Pan and others 2016). We also found a strong and consistent positive correlation between Fe(II) and DOC in water samples from the SPRUCE enclosure outlets and S2 near-surface porewater (Figure 3A, C, Table 1). Although many factors such as temperature, enzyme activity, and C composition influence peatland DOC release (Freeman and others 2001; Riedel and others 2014), our results suggest that Fe(III) reduction promoted at least part of the DOC loss from the bogs and contributed to a positive correlation between Fe(II) and DOC. As discussed later, protective complexation of Fe(II) by DOC also likely contributed to the correlation. Other potential mechanisms include evaporative concentration of ions, organic matter decomposition, or non-specific electrostatic interactions. However, our data suggest that these other mechanisms are not likely principal drivers of the observed relationship between Fe and C.

Four arguments support the hypothesis that Fe(III) reduction contributed to the observed correlation between Fe(II) and DOC in water samples. First, Fe(II) did not show the same response to temperature treatments as the non-redox-active cations, which we would expect in the case of non-specific electrostatic interactions (i.e., if charge balance alone controlled the cation/DOC relationship) or evaporative concentration. There was a weak positive correlation between Cl and DOC in the SPRUCE water samples but not in the ambient S2 samples (Figure S5), indicating that evaporative concentration had only a minor influence on the relationship between DOC and ions. The stronger relationship between Na and DOC than Cl and DOC suggests that electrostatic interactions contributed to correlations between cations and DOC, but differing relationships of regression slopes with temperature among the different cations also suggest that charge balance alone cannot explain the Fe(II)/DOC relationship. Both Ca and Na were also positively correlated with DOC in the water samples, but the slope of the correlation changed among SPRUCE temperature treatments (Figures 3B and S4a). In contrast, the Fe(II)/DOC slope did not significantly change among temperature treatments (Figure 3A) despite greater evapotranspiration at higher temperature (Hanson and others 2020a). The difference between Fe(II) and Ca in response to temperature was also demonstrated by changes in Fe(II)/Ca molar ratios in SPRUCE outflow water samples among temperature treatments (Figure S9). If Fe(II) responded in the same way as Ca to increased temperature, their molar ratio would be consistent among treatments. Second, we found a spatial difference between the relationships of Fe(II)/DOC and Ca/DOC. In the S2 bog near-surface porewater samples, the correlation between DOC and Ca varied among water sampling sites but the correlation between DOC and Fe was similar for the three sites (Figure 3C, D). This difference in Ca/DOC slope by site could be due to variable dis-

tances of bog sampling locations from the lagg, which receives Ca-rich water from the uplands. Third, elemental stoichiometry of the bog vegetation implies that increased decomposition at warmer temperatures cannot solely explain Fe/DOC relationships. The average plant foliage tissue in the S1 bog had a Ca/Fe molar ratio of 23 (Phillips and others 2017), but the Ca/Fe molar ratio averaged 1.2 across the SPRUCE outflow samples. The increased concentration of Fe in outflow samples from the warmed enclosures was much higher than it would be if it were strictly provided from litter decomposition, in which case we would expect similar Ca/Fe ratios in water samples and intact biomass. Increased decomposition of surface peat under warming treatments could in principle release soluble complexes of DOC and Fe(II) or DOC and Ca, but again, this would not explain the differing responses of Fe(II) and Ca to temperature (Figure S9). Fourth, we often observed a significant release of Ca and Mg when Fe(III) was reduced in the dithionite + HCl extractions (Figure 2), suggesting that Fe(III) reduction released occluded cations as well as DOC. That is, cations bound to organic matter that was physically or chemically associated with Fe may also have been released when Fe(III) was reduced (Hall and Huang 2017). Via release of occluded cations, the reduction of Fe(III) could contribute at least partly to the correlation between DOC and Ca.

In addition to these arguments, we can compare C/Fe molar ratios from peat extractions and water samples to estimate the proportion of DOC in stream outflow that may have resulted from Fe(III) reduction. The slope of the molar relationship between Fe-associated C and Fe(III) was 13 in peat from 0 to 50 cm, the depth where Fe-associated C was measurable (Figure S10). For comparison, the mean molar ratio of Fe-associated C/Fe(III) of the 30 soil samples from Wagai and Mayer (2007) was 2.1 (calculated from their supplemental data). The large differences in these ratios likely derive from differences in DOC molecular composition and its direct and indirect associations with Fe(III) in peatlands vs. mineral soils. The slopes of the molar relationship between DOC and Fe(II) in SPRUCE water and S2 near-surface porewater were 92 and 105, respectively (Figure 3A, C). Comparing the ratio of C/Fe released in the peat extractions (Figure S10) with the water samples indicates that approximately 12–14% of C lost in stream or enclosure outflow could directly result from Fe(III) reduction. However, this estimate is conservative. Iron reduction and oxidation cycling may also contribute to additional DOC release indirectly through pH changes (Grybos and others 2009), by serving as an electron acceptor and enhancing overall decomposition and C depolymerization rates, and by producing reactive oxygen species that depolymerize particulate C to DOC (Chen and others 2020). These mechanisms likely further contributed to the very tight coupling between Fe(II) and DOC in water samples (R^2 = 0.56–0.78) beyond what could be directly explained by release of Fe-bound C.

Fe as a Passenger in the Fe–DOC Relationship

Although Fe(III) reduction likely contributed to the strong correlation between Fe(II) and DOC, DOC also likely facilitated Fe(II) export. DOC may complex Fe(II) and slow the oxidation of Fe(II) to Fe(III) (Theis and Singer 1974; Daugherty and others 2017). Accordingly, Fe(II) can persist even in oxygenated stream water, where it would otherwise be expected to oxidize to Fe(III) (Gaffney and others 2008), and Fe(II) associated with DOC has been observed in oxygenated freshwater lakes (von der Heyden and others 2014). This mechanism is consistent with our findings that DOC positively correlated with Fe(II) but not Fe(III) (Figures 3A, C and S3) in variably oxygenated water where Fe(II) would be expected to slowly oxidize. However, these findings may be dependent on the location of the sampling, as Fe(II) might oxidize to Fe(III) farther downstream even when complexed by DOC. Regardless of its ultimate fate, Fe was dominantly exported from these peatlands as Fe(II), perhaps due to protective complexation by DOC, and thus, Fe was likely both a passenger as well as a driver of DOC loss following Fe(III) reduction.

Fe Reduction Releases SRP

In addition to DOC, Fe(III) reduction also released small amounts of P, a limiting nutrient in bogs (Bridgham and others 1996; Hill and others 2014). There was a small net release of P following Fe(III) chemical reduction in 0–30 cm peat (Figure 2E), consistent with other recent work at the S1 and S2 bogs (Herndon and others 2019). The Fe-associated P in 0–20 cm peat (3.0 ± 0.6 μmol g^{-1}; Figures 2E and S2) was smaller than reported by Herndon and others (2019) (10 ± 0.2 μmol g^{-1} and 7 ± 1 μmol g^{-1} in peat hollows from the S1 and S2 bog, respectively, calculated from their supplemental material), but we used a more conservative extraction method that accounted for ion-

exchangeable P. Furthermore, we found that P was not only associated with Fe, but that it was increasingly released under elevated temperature. We observed a positive correlation between SRP and Fe(II) at warmer but not cooler SPRUCE temperature treatments, and we found a negative correlation in the S2 near-surface porewater (Figure S6a, b). The lack of positive correlation in the latter treatments may reflect P limitation. Where P is limiting, it may be quickly assimilated and therefore was not present in the outflow water samples. One explanation for the positive correlation between SRP and Fe(II) at warmer temperatures may be that P release exceeded immediate biological uptake.

The Influence of Temperature and Water Elevation on Fe(III) Reduction

Temporal variation in Fe(II) concentrations in water samples could be predicted by temperature, moisture, and their interaction (Figure 6). We found a nonlinear response of Fe(II) concentration to SPRUCE nominal temperature treatments (Figure 4A) suggesting that Fe(III) reduction initially increased with temperature but eventually reached a plateau. The plateau at the highest temperature treatment was likely due to lower Fe(III) reduction resulting from decreased soil moisture, as indicated by the significant temperature x water depth interaction in the GAMM (Figure 6). Our results demonstrate the strong temperature sensitivity of Fe(III) reduction under field conditions, building on previous laboratory experiments (Yao and Conrad 2000; Meier and others 2005; Schilling and others 2019). Therefore, all else equal, we would expect rising temperatures to increase Fe(III) reduction and promote the hydrologic efflux of Fe(II), DOC, and associated nutrients. However, due to increased evapotranspiration and lower water depths (Hanson and others 2020a), warmer temperatures may ultimately suppress Fe(III) reduction as peats become drier for longer durations. Water table levels may also affect Fe/DOC relationships by influencing DOC composition (Tfaily and others 2018), as certain C compounds are likely to coprecipitate with or be released by Fe (Riedel and others 2013, 2014). Our results demonstrate that temperature and moisture can be used to predict Fe(III) reduction rates in peatlands, highlighting that these factors should be included in ecosystem models for this biome (Shi and others 2015). Finally, we note that even in these frequently flooded systems, Fe was not necessarily reduced simply because water levels were high; temperature was key in controlling the Fe oxidation state.

Broader Implications for Peatland Carbon Dynamics

We showed that Fe redox cycling is a potentially important gatekeeper of DOC and nutrients in a mineral-poor ecosystem where DOC is an important component of the C budget and mineral nutrients may be strongly limiting. In peatlands, DOC export through streams can be a large C loss. For example, the mean TOC efflux in the S1 bog represented 37% of mean net ecosystem production and was similar to CH_4 efflux (Griffiths and others 2017). This percentage is not uncommon, as peatlands in Canada, Sweden, Scotland, and Ireland also had TOC or DOC effluxes ranging from 24 to 37% of net ecosystem exchange (Roulet and others 2007; Nilsson and others 2008; Dinsmore and others 2010; Koehler and others 2011). Not only can Fe redox cycling influence DOC export, but it is sensitive to changes in temperature and moisture expected with global change. If warmer temperatures increase Fe(III) reduction, an even larger percentage of NEP could be lost as TOC. We found that Fe(III)-bound C averaged 270 g C m^{-2}, much greater than the annual TOC efflux of 14.2 g C m^{-2} y^{-1} from the S1 bog (Griffiths and others 2017). Therefore, variation in Fe(III)-bound C is large enough, in principle, to impact DOC efflux over decadal scales. In addition to influencing DOC efflux through stream export, Fe(III) reduction can also directly or indirectly catalyze decomposition to CO_2 and CH_4 (Chen and others 2020), and likely contributes to increased emissions of these gases from warmed peatlands (Hanson and others 2020a; Hopple and others 2020). Even in ecosystems such as our study bogs, which are largely devoid of minerals, redox-active metals may play key and underappreciated roles in mediating ecosystem processes.

ACKNOWLEDGEMENTS

We thank two anonymous reviewers and Keith Oleheiser, Anne Gapinski, Anthony Mirabito, and Toni Sleugh for assistance. This paper leverages several publicly available datasets cited in the text. This research was supported in part by startup funds to SJH from Iowa State University. NAG was supported by the U.S. Department of Energy (DOE), Office of Science, Office of Biological and Environmental Research. Oak Ridge National Laboratory (ORNL) is managed by UT-Battelle, LLC,

for the U.S. Department of Energy under contract DE-AC05-00OR22725. The U.S. DOE SPRUCE was constructed and is operated by ORNL. SPRUCE research is a collaborative effort between ORNL and the USDA Forest Service. The participation of SDS in SPRUCE efforts, monitoring data from the MEF, sampling, and associated water chemistry analyses were funded by the Northern Research Station of the USDA Forest Service.

REFERENCES

Björnerås C, Weyhenmeyer GA, Evans CD, Gessner MO, Grossart H-P, Kangur K, Kokorite I, Kortelainen P, Laudon H, Lehtoranta J, Lottig N, Monteith DT, Nõges P, Nõges T, Oulehle F, Riise G, Rusak JA, Räike A, Sire J, Sterling S, Kritzberg ES. 2017. Widespread increases in iron concentration in European and North American freshwaters. Glob Biogeochem Cycles 31:1488–1500.

Blazevic A, Orlowska E, Kandioller W, Jirsa F, Keppler BK, Tafili-Kryeziu M, Linert W, Krachler RF, Krachler R, Rompel A. 2016. Photoreduction of terrigenous Fe-humic substances leads to bioavailable iron in oceans. Angew Chem 128:6527–6532.

Blodau C, Roehm CL, Moore TR. 2002. Iron, sulfur, and dissolved carbon dynamics in a northern peatland. Arch Hydrobiol 154(4):561–583.

Bridgham SD, Pastor J, Janssens JA, Chapin C, Malterer TJ. 1996. Multiple limiting gradients in peatlands: a call for a new paradigm. Wetlands 16:45–65.

Chacon N, Silver WL, Dubinsky EA, Cusack DF. 2006. Iron reduction and soil phosphorus solubilization in humid tropical forests soils: the roles of labile carbon pools and an electron shuttle compound. Biogeochemistry 78:67–84.

Chen J, Gu B, Royer RA, Burgos WD. 2003. The roles of natural organic matter in chemical and microbial reduction of ferric iron. Sci Total Environ 307:167–178.

Chen C, Meile C, Wilmoth J, Barcellos D, Thompson A. 2018. Influence of pO_2 on iron redox cycling and anaerobic organic carbon mineralization in a humid tropical forest soil. Environ Sci Technol 52:7709–7719.

Chen C, Hall SJ, Coward E, Thompson A. 2020. Iron-mediated organic matter decomposition in humid soils can counteract protection. Nat Commun 11:1–13.

Chin Y-P, Traina SJ, Swank CR, Backhus D. 1998. Abundance and properties of dissolved organic matter in pore waters of a freshwater wetland. Limnol Oceanogr 43:1287–1296.

Curtinrich HJ, Hall SJ, Sebestyen SD. 2021. Marcell Experimental Forest peat core extraction chemical analysis data (DOC, Fe, Ca, Mg, K, P, Al) ver 1. Environmental Data Initiative. https://doi.org/10.6073/pasta/8c2c908fec929b5fd812851ef9150301

Daugherty EE, Gilbert B, Nico PS, Borch T. 2017. Complexation and redox buffering of iron(II) by dissolved organic matter. Environ Sci Technol 51:11096–11104.

Dinsmore KJ, Billett MF, Skiba UM, Rees RM, Drewer J, Helfter C. 2010. Role of the aquatic pathway in the carbon and greenhouse gas budgets of a peatland catchment. Glob Change Biol 16:2750–2762.

Eisenreich SJ, Hollod GJ, Langevin S. 1978. Precipitation chemistry and atmospheric deposition of trace elements in Northeastern Minnesota. Minneapolis, MN: Environmental Engineering Program, Dept. of Civil and Mineral Engineering, University of Minnesota.

Ekström SM, Regnell O, Reader HE, Nilsson PA, Löfgren S, Kritzberg ES. 2016. Increasing concentrations of iron in surface waters as a consequence of reducing conditions in the catchment area. J Geophys Res Biogeosci 121:479–493.

Freeman C, Evans CD, Monteith DT, Reynolds B, Fenner N. 2001. Export of organic carbon from peat soils. Nature 412:785–785.

Gaffney JW, White KN, Boult S. 2008. Oxidation state and size of Fe controlled by organic matter in natural waters. Environ Sci Technol 42:3575–3581.

Griffiths NA, Sebestyen SD. 2016. Dynamic vertical profiles of peat porewater chemistry in a northern peatland. Wetlands 36:1119–1130.

Griffiths NA, Hanson PJ, Ricciuto DM, Iversen CM, Jensen AM, Malhotra A, McFarlane KJ, Norby RJ, Sargsyan K, Sebestyen SD, Shi X, Walker AP, Ward EJ, Warren JM, Weston DJ. 2017. Temporal and spatial variation in peatland carbon cycling and implications for interpreting responses of an ecosystem-scale warming experiment. Soil Sci Soc Am J 81:1668–1688.

Griffiths NA, Sebestyen SD, Oleheiser KC. 2019. Variation in peatland porewater chemistry over time and space along a bog to fen gradient. Sci Total Environ 697:134152.

Grybos M, Davranche M, Gruau G, Petitjean P, Pédrot M. 2009. Increasing pH drives organic matter solubilization from wetland soils under reducing conditions. Geoderma 154:13–19.

Hagedorn F, Kaiser K, Feyen H, Schleppi P. 2000. Effects of redox conditions and flow processes on the mobility of dissolved organic carbon and nitrogen in a forest soil. J Environ Qual 29:288–297.

Hall SJ, Huang W. 2017. Iron reduction: a mechanism for dynamic cycling of occluded cations in tropical forest soils? Biogeochemistry 136:91–102.

Hall SJ, Treffkorn J, Silver WL. 2014. Breaking the enzymatic latch: impacts of reducing conditions on hydrolytic enzyme activity in tropical forest soils. Ecology 95:2964–2973.

Hanson P, Riggs J, Nettles W, Krassovski M, Hook L. 2016. SPRUCE whole ecosystems warming (WEW) environmental data beginning August 2015. Oak Ridge, TN: Oak Ridge Natl Lab, TES SFA, US Dept Energy. https://doi.org/10.3334/CDIAC/spruce.032

Hanson PJ, Riggs JS, Nettles WR, Phillips JR, Krassovski MB, Hook LA, Gu L, Richardson AD, Aubrecht DM, Ricciuto DM, Warren JM, Barbier C. 2017. Attaining whole-ecosystem warming using air and deep-soil heating methods with an elevated CO_2 atmosphere. Biogeosciences 14:861–883.

Hanson PJ, Griffiths NA, Iversen CM, Norby RJ, Sebestyen SD, Phillips JR, Chanton JP, Kolka RK, Malhotra A, Oleheiser KC, Warren JM, Shi X, Yang X, Mao J, Ricciuto DM. 2020a. Rapid net carbon loss from a whole-ecosystem warmed peatland. AGU Adv 1:e2020AV000163.

Hanson PJ, Phillips JR, Nettles WR, Pearson KJ, Hook LA. 2020b. SPRUCE plot-level water table data assessments for absolute elevations and height with respect to mean hollows beginning in 2015. Oak Ridge, TN: Oak Ridge Natl Lab, TES SFA, US Dept Energy. https://doi.org/10.25581/spruce.079/1608615.

Herndon EM, Kinsman-Costello L, Duroe KA, Mills J, Kane ES, Sebestyen SD, Thompson AA, Wullschleger SD. 2019. Iron (oxyhydr)oxides serve as phosphate traps in tundra and boreal peat soils. J Geophys Res Biogeosci 124:227–246.

Hill BH, Elonen CM, Jicha TM, Kolka RK, Lehto LLP, Sebestyen SD, Seifert-Monson LR. 2014. Ecoenzymatic stoichiometry and microbial processing of organic matter in northern bogs and fens reveals a common P-limitation between peatland types. Biogeochemistry 120:203–224.

Hopple AM, Wilson RM, Kolton M, Zalman CA, Chanton JP, Kostka J, Hanson PJ, Keller JK, Bridgham SD. 2020. Massive peatland carbon banks vulnerable to rising temperatures. Nat Commun 11:2373.

Huang W, Hall SJ. 2017b. Optimized high-throughput methods for quantifying iron biogeochemical dynamics in soil. Geoderma 306:67–72.

Huang W, Hall SJ. 2017a. Elevated moisture stimulates carbon loss from mineral soils by releasing protected organic matter. Nat Commun 8:1774.

Iversen C, Hanson P, Brice D, Phillips J, McFarlane K, Hobbie E, Kolka R. 2014. SPRUCE peat physical and chemical characteristics from experimental plot cores, 2012. Oak Ridge, TN: Oak Ridge Natl Lab, TES SFA, US Dept Energy. https://doi.org/10.3334/CDIAC/spruce.005

Keller JK, Bridgham SD. 2007. Pathways of anaerobic carbon cycling across an ombrotrophic-minerotrophic peatland gradient. Limnol Oceanogr 52:96–107.

Keller JK, Takagi KK. 2013. Solid-phase organic matter reduction regulates anaerobic decomposition in bog soil. Ecosphere 4:art54.

Kleber M, Eusterhues K, Keiluweit M, Mikutta C, Mikutta R, Nico PS. 2015. Mineral–organic associations: formation, properties, and relevance in soil environments. Adv Agron 130:1–140.

Knorr K-H. 2013. DOC-dynamics in a small headwater catchment as driven by redox fluctuations and hydrological flow paths—are DOC exports mediated by iron reduction/oxidation cycles? Biogeosciences 10:891–904.

Koehler A-K, Sottocornola M, Kiely G. 2011. How strong is the current carbon sequestration of an Atlantic blanket bog? Glob Change Biol 17:309–319.

Kolka RK, Sebestyen SD, Verry ES, Brooks KN, Eds. 2011. Peatland biogeochemistry and watershed hydrology at the Marcell Experimental Forest. Boca Raton, FL: CRC Press.

Küsel K, Blöthe M, Schulz D, Reiche M, Drake HL. 2008. Microbial reduction of iron and porewater biogeochemistry in acidic peatlands. Biogeosciences 5:1537–1549.

Lovley DR, Phillips EJP. 1987. Rapid assay for microbially reducible ferric iron in aquatic sediments. Appl Environ Microbiol 53:1536–1540.

McKnight DM, Bencala KE. 1990. The chemistry of iron, aluminum, and dissolved organic material in three acidic, metal-enriched, mountain streams, as controlled by watershed and in-stream processes. Water Resour Res 26:3087–3100.

Meier J, Costa R, Smalla K, Boehrer B, Wendt-Potthoff K. 2005. Temperature dependence of Fe(III) and sulfate reduction rates and its effect on growth and composition of bacterial enrichments from an acidic pit lake neutralization experiment. Geobiology 3:261–274.

Neal C, Lofts S, Evans CD, Reynolds B, Tipping E, Neal M. 2008. Increasing iron concentrations in UK upland waters. Aquat Geochem 14:263–288.

Nilsson M, Sagerfors J, Buffam I, Laudon H, Eriksson T, Grelle A, Klemedtsson L, Weslien P, Lindroth A. 2008. Contemporary carbon accumulation in a boreal oligotrophic minerogenic mire—a significant sink after accounting for all C-fluxes. Glob Change Biol 14:2317–2332.

Oni SK, Futter MN, Bishop K, Köhler SJ, Ottosson-Löfvenius M, Laudon H. 2013. Long-term patterns in dissolved organic carbon, major elements and trace metals in boreal headwater catchments: trends, mechanisms and heterogeneity. Biogeosciences 10:2315–2330.

Pan W, Kan J, Inamdar S, Chen C, Sparks D. 2016. Dissimilatory microbial iron reduction release DOC (dissolved organic carbon) from carbon-ferrihydrite association. Soil Biol Biochem 103:232–240.

Phillips JR, Brice DJ, Hanson PJ, Childs J, Iversen CM, Norby RJ, Warren JM. 2017. SPRUCE pretreatment plant tissue analyses, 2009 through 2013. Oak Ridge, TN: Oak Ridge Natl Lab, TES SFA, US Dept Energy. https://doi.org/10.3334/CDIAC/spruce.038

Riedel T, Zak D, Biester H, Dittmar T. 2013. Iron traps terrestrially derived dissolved organic matter at redox interfaces. Proc Natl Acad Sci 110:10101–10105.

Riedel T, Iden S, Geilich J, Wiedner K, Durner W, Biester H. 2014. Changes in the molecular composition of organic matter leached from an agricultural topsoil following addition of biomass-derived black carbon (biochar). Org Geochem 69:52–60.

Roulet NT, Lafleur PM, Richard PJH, Moore TR, Humphreys ER, Bubier J. 2007. Contemporary carbon balance and late Holocene carbon accumulation in a northern peatland. Glob Change Biol 13:397–411.

Schilling K, Borch T, Rhoades CC, Pallud CE. 2019. Temperature sensitivity of microbial Fe(III) reduction kinetics in subalpine wetland soils. Biogeochemistry 142:19–35.

Sebestyen SD, Griffiths NA. 2016. SPRUCE enclosure corral and sump system: description, operation, and calibration. Oak Ridge, TN: Clim Change Sci Inst Oak Ridge Natl Lab US Dept Energy. https://doi.org/10.3334/CDIAC/spruce.030

Sebestyen SD, Verry ES, Brooks KN. 2011b. Hydrological responses to changes in forest cover on uplands and peatlands. In: Kolka RK, Sebesteyen SD, Verry ES, Brooks KN, Eds. Peatland biogeochemistry and watershed hydrology at the Marcell Experimental Forest, . Boca Raton, FL: CRC Press. pp 401–432.

Sebestyen SD, Dorrance C, Olson D, Verry ES, Kolka RK, Elling AE, Kyllander R. 2011a. Long-term monitoring sites and trends at the Marcell Experimental Forest. In: Kolka RK, Sebestyen SD, Verry ES, Brooks K, Eds. Peatland biogeochemistry and watershed hydrology at the Marcell Experimental Forest, . Boca Raton, FL: CRC Press. pp 15–71.

Sebestyen SD, Funke MM, Cotner JB, Larson JT, Aspelin NA. 2020a. Water chemistry data for studies of the biodegradability of dissolved organic matter in peatland catchments at the Marcell Experimental Forest: 2009–2011. Fort Collins CO: Forest Service Research Data Archive. Updated 16 May 2020. https://doi.org/10.2737/RDS-2017-0067

Sebestyen SD, Oleheiser KC, Larson JT, Aspelin NA, Stelling JM, Griffiths NA, Lany NK. 2020b. Marcell Experimental Forest event based precipitation chemistry, 2008—ongoing. https://portal.edirepository.org/nis/mapbrowse?packageid=edi.609.1. Last accessed 05/03/2021

Sebestyen SD, Verry ES, Elling AE, Kyllander RL, Roman DT, Burdick JM, Lany NK, Kolka RK. 2020c. Marcell Experimental Forest daily precipitation, 1961—ongoing. https://portal.edirepository.org/nis/mapbrowse?packageid=edi.563.1. Last accessed 05/03/2021

Sebestyen SD, Funke M, Cotner JB. 2021a. Sources and biodegradability of dissolved organic matter in two headwater peatland catchments at the Marcell Experimental Forest, northern Minnesota, USA. Hydrol Process 35:e14049.

Sebestyen SD, Lany NK, Roman DT, Burdick JM, Kyllander RL, Verry ES, Kolka RK. 2021b. Hydrological and meteorological data from research catchments at the Marcell Experimental Forest. Hydrol Process. https://doi.org/10.1002/hyp.14092. In Press.

Sebestyen SD, Lany NK, Larson JT, Aspelin NA, Oleheiser KC, Nelson DK, Hall SJ, Curtinrich HJ. 2021c. Marcell Experimental Forest porewater chemistry at the S2 catchment, 2009—ongoing ver 2. Environmental Data Initiative. https://doi.org/10.6073/pasta/d7d5a29015ede8f226166064bc41cb87.

Sebestyen SD, Griffiths NA, Oleheiser KC, Stelling JM, Pierce CE, Nater EA, Wilson RM, Chanton JP, Hall SJ, Curtinrich HJ, Toner BM, Kolka RK. 2021d. SPRUCE outflow chemistry data for experimental plots beginning in 2016. Oak Ridge National Laboratory, TES SFA, U.S. Department of Energy, Oak Ridge, Tennessee, U.S.A. https://doi.org/10.25581/spruce.088/1775142.

Senesi N, Griffith SM, Schnitzer M, Townsend MG. 1977. Binding of Fe^{3+} by humic materials. Geochim Cosmochim Acta 41:969–976.

Shi X, Thornton PE, Ricciuto DM, Hanson PJ, Mao J, Sebestyen SD, Griffiths NA, Bisht G. 2015. Representing northern peatland microtopography and hydrology within the Community Land Model. Biogeosciences 12:6463–6477.

Tfaily MM, Wilson RM, Cooper WT, Kostka JE, Hanson P, Chanton JP. 2018. Vertical stratification of peat pore water dissolved organic matter composition in a peat bog in Northern Minnesota. J Geophys Res Biogeosci 123:479–494.

Theis TL, Singer PC. 1974. Complexation of iron(II) by organic matter and its effect on iron(II) oxygenation. Environ Sci Technol 8:569–573.

Thompson A, Chadwick OA, Boman S, Chorover J. 2006. Colloid mobilization during soil iron redox oscillations. Environ Sci Technol 40:5743–5749.

Urban NR, Eisenreich SJ, Gorham E. 1987. Aluminum, iron, zinc, and lead in bog waters of northeastern North America. Can J Fish Aquat Sci 44:1165–1172.

Urban N, Verry ES, Eisenreich S, Grigal D, Sebestyen S. 2011. Element cycling in upland/peatland watersheds. In: Kolka RK, Sebestyen SD, Verry ES, Brooks KN, Eds. Peatland biogeochemistry and watershed hydrology at the Marcell Experimental Forest, . Boca Raton, FL: CRC Press. pp 213–241.

Verry ES. 1975. Streamflow chemistry and nutrient yields from upland-peatland watersheds in Minnesota. Ecology 56:1149–1157.

Verry ES, Janssens J. 2011. Geology, vegetation, and hydrology of the S2 bog at the MEF: 12,000 years in Northern Minnesota. In: Kolka RK, Sebesteyen SD, Verry ES, Brooks KN, Eds. Peatland biogeochemistry and watershed hydrology at the Marcell Experimental Forest, . Boca Raton, FL: CRC Press. pp 93–134.

Verry ES, Brooks KN, Nichols DS, Ferris DR, Sebestyen SD. 2011. Watershed hydrology. In: Kolka RK, Sebestyen SD, Verry ES, Brooks KN, Eds. Peatland biogeochemistry and watershed hydrology at the Marcell Experimental Forest, . Boca Raton, FL: CRC Press. pp 193–212.

von der Heyden BP, Hauser EJ, Mishra B, Martinez GA, Bowie AR, Tyliszczak T, Mtshali TN, Roychoudhury AN, Myneni SCB. 2014. Ubiquitous presence of Fe(II) in aquatic colloids and its association with organic carbon. Environ Sci Technol Lett 1:387–392.

Wagai R, Mayer LM. 2007. Sorptive stabilization of organic matter in soils by hydrous iron oxides. Geochim Cosmochim Acta 71:25–35.

Weyhenmeyer GA, Prairie YT, Tranvik LJ. 2014. Browning of boreal freshwaters coupled to carbon-iron interactions along the aquatic continuum. Iwata T, editor. PLoS ONE 9:e88104.

Wood S. 2006. Generalized additive models: an introduction with R/Simon N. Wood. Boca Raton, FL: Chapman & Hall/CRC.

Yao H, Conrad R. 2000. Effect of temperature on reduction of iron and production of carbon dioxide and methane in anoxic wetland rice soils. Biol Fertil Soils 32:135–141.

Zhao Q, Poulson SR, Obrist D, Sumaila S, Dynes JJ, McBeth JM, Yang Y. 2016. Iron-bound organic carbon in forest soils: quantification and characterization. Biogeosciences 13:4777–4788.